

## Synthesis and evaluation of chitosan manganese-ferrite nanoparticles as MRI contrast agent

S. Rasaneh<sup>1\*</sup>; M. Raheleh Dadras<sup>2</sup>

<sup>1</sup> Nuclear Sciences and Technology Research Institute, Tehran

<sup>2</sup> International Campus, Iran University of Medical Sciences, Tehran

Received: 6 June 2015; Accepted: 9 August 2015

---

**ABSTRACT:** Magnetic nanoparticles are the good choice for using in MRI as the contrast agent. Iron oxide particles such as magnetite ( $\text{Fe}_3\text{O}_4$ ) or its oxidized form maghemite ( $\gamma\text{-Fe}_2\text{O}_3$ ) are the most commonly employed in biomedical applications. In this study, we synthesized and optimized the preparation of chitosan manganese-ferrite nanoparticles (CMn-Fe nps) and evaluated its ability for the mice macrophage cells imaging with MRI. The core and hydrodynamic size of the nanoparticles was  $54\pm 27$  nm and  $149\pm 48$  nm respectively. The magnetization reached a saturation magnetization value of 95 emu/g. The MRI images showed that the liver and some other organs were accumulated the CMn-Fe nps and produced a negative contrast in images. CMn-Fe nps demonstrated that it is a good candidate for using as a contrast agent material in macrophage cells imaging with MRI.

**Keywords:** Chitosan; Contrast agent; Manganese ferrite nanoparticles; MRI imaging

---

## INTRODUCTION

Magnetic particles from nanometer to micrometer size have been widely used in biological and medical fields (Ito, *et al.*, 2005). Magnetic particles have good response to magnetic force and magnetic nanoparticles show superparamagnetic behavior at room temperature that does not retain any magnetism after removal of the magnetic field. The applications of magnetic nanoparticles for imaging are: gastrointestinal tract imaging, detecting liver and spleen disease, kidney imaging, detecting lymph node metastases, blood pool characteristics, phagocytosis imaging, and etc. (Ito, *et al.*, 2005). Furthermore, the particles must have combined properties of high magnetic saturation, biocompatibility and

interactive functions at the surfaces (Thorek, *et al.*, 2006). Iron oxide particles such as magnetite ( $\text{Fe}_3\text{O}_4$ ) or its oxidized form maghemite ( $\gamma\text{-Fe}_2\text{O}_3$ ) are the most commonly employed in biomedical applications since their biocompatibility has already been proven (Gupta and Gupta 2005). The applications of MRI have steadily increased over the past decade. MRI offers the advantage of high spatial resolution and contrast differences between tissues. Due to the unique function of this imaging modality, there is a need to develop effective contrast agents that will enhance and widen its diagnostic utility (Thorek, *et al.*, 2006). Manganese ferrite ( $\text{MnFe}_2\text{O}_4$ ) nanoparticles are useful for remarkable soft-magnetic properties (low coercivity, moderate saturation magnetization) accompanied by good

---

(\*) Corresponding Author - e-mail: srasaneh@aeoi.org.ir

chemical stability and mechanical hardness (Rasaneh and Dadras 2014). Uncoated magnetic nanoparticles aggregate in biological solutions due to their large surface area to volume ratio, forming large clusters and rendering them unsuitable for biomedical applications. Therefore, an appropriate coating is needed to reduce the surface free energy in order to protect the nanoparticles aggregate against agglomeration. The polymer coating not only inhibits aggregation and increases stability but also leads to the creation of more hydrophilic nanostructures and provides a variety of surface functional groups to bind drug molecules. Non-toxic and biodegradable polymers such as chitosan have been used extensively in biomedical fields (Wang, *et al.*, 2011, Dung, *et al.*, 2009). Chitosan is a linear polysaccharide comprised of two monosaccharides: N-acetyl-D-glucosamine and D-glucosamine linked together by glucosidic bonds. Chitosan has 1 primary amino and 2 free hydroxyl groups for each C6 building unit (Banerjee, *et al.*, 2002). In recent researches, the magnetite chitosan NPs were obtained by crosslinking of chitosan amino groups using glutaraldehyde (Patil, *et al.*, 2014, Qu, *et al.*, 2010). The disadvantage of this method is the toxicity of this crosslinker (Hritcu, *et al.*, 2009). Ionic gelation (polyionic coacervation) is an interesting technique that uses non-toxic poly-anions, such as sodium tripolyphosphate (TPP) as non-toxic ionic crosslinker. This method is simple and reproducible and NPs are encapsulated in a chitosan shell by ionic interactions (Hritcu, *et al.*, 2009). In this study, we synthesized and optimized the preparation of chitosan manganese-ferrite nanoparticles (CMn-Fe nps) and evaluated its ability for the mice macrophage cells imaging with MRI.

## MATERIALS AND METHODS

### Materials

Ferric chloride ( $\text{FeCl}_3$ ), manganese chloride ( $\text{MnCl}_2 \cdot 4\text{H}_2\text{O}$ ), ammonia solution (25% wt), Water-soluble chitosan (Low molecular weight, 97% deacetylated) and Sodium tripolyphosphate (TPP) were purchased from Sigma Co. All salts and buffers used in this study were of reagent grade and purchased from Fluka chemical corp.

### Synthesis

50 mL of  $\text{FeCl}_3 \cdot 6\text{H}_2\text{O}$  (0.32 M) and 50 mL of  $\text{MnCl}_2 \cdot 4\text{H}_2\text{O}$  (0.2 M) were mixed in the reactor. Then, 0.125 gr of chitosan was added to the solution and the temperature was raised to  $70^\circ\text{C}$ . Precipitation was initiated by addition of 20 mL of the aqueous  $\text{NH}_4\text{OH}$  at 0.5 mL/min. Then, the completion reaction was allowed to proceed for 60 min. The nanoparticles were washed with Q water several times by using a permanent magnet, separated in desired size by centrifugation in 10000 rpm and lyophilized to obtain the final product (Rasaneh, *et al.*, 2011, Kueny-Stotz, *et al.*, 2012).

### Physical characteristics

For determining the amounts of iron content in the Mn-Fe nps used colorimetric assay. A sample (100  $\mu\text{L}$ ) of nanoparticles was mixed with HCl (100  $\mu\text{L}$ ) and  $\text{H}_2\text{O}_2$  (10%, 100  $\mu\text{L}$ ) to allow the iron content of nanoparticles be dissolved and oxidized to  $\text{Fe}^{3+}$ . After adding potassium thiocyanate (3%, 1 mL), the  $\text{Fe}^{3+}$  formed a red complex with the thiocyanate which could be measured by a spectrophotometer at 480 nm (2100 UV spectrophotometer, UNICO Instruments, China). The standard curve for calculation of iron content was obtained measuring different concentrations (0, 250, 500 and 1,000  $\mu\text{g}/\text{mL}$ ) of ferric chloride (Rasaneh, *et al.*, 2011). The hydrodynamic sizes of the particles were measured using a dynamic light scattering (DLS) device from Malvern Instruments (model HPPS). The mean sizes were determined with independent measurements from three drawn samples of the preparation with 5 runs per sample, 15 determinations in total. The core sizes of nanoparticles were also determined by Transmission Electronic Microscopy (TEM) (JEM 2010, JEOL, JAPAN). Magnetization measurements were performed using an MPMS-XL superconducting quantum interference device (SQUID) magnetometer (Quantum Design Inc., San Diego, CA). The freeze-dried samples of Mn-Fe nps (5-6 mg Fe) were analyzed in a DC magnetic field range of 0–55 kG.

### MRI study

The male bulb/c mice ( $n=6$ , 6-8 weeks old, 25-30 g) were obtained and housed under pathogen free conditions and fed with autoclaved food and water. Mice

received a dose of 100  $\mu\text{g}$  (100  $\mu\text{L}$ ) of Mn-Fe nps by the tail vein injection. MR imaging of the animals ( $n=3$ ) were performed before and 4 hours after injection of Mn-Fe nps. The animals were anesthetized and fixed in the same position. Imaging was performed with 1.5 Tesla MR imaging (SIEMENS, Symphony) and a knee coil. Pulse sequence comprised coronal T2-weighted three-dimensional fast field-echo, 32/10 sequences with a flip angle of 250 and effective section thickness of 650  $\mu\text{m}$ . For better comparison, at before, 10 minutes and 4 hours after injection, the mice were scarified, organs removed, washed and put in saline buffer and imaged with MRI.

## RESULTS AND DISCUSSION

### Particle characterization

The magnetic responsiveness of Mn-Fe nps in solution was visualized by a simple experiment in which a 0.40 T magnet was placed near the glass vials (Fig. 1). The Mn-Fe nps deposited notably on the wall adjacent to the magnet within 1 minute.

The average core size of nanoparticles measured by TEM was  $54\pm 27$  nm that is shown in Fig. 2-A. The hydrodynamic size of the Mn-Fe nps that determined by DLS technique was  $149\pm 48$  nm and the particles distribution is presented in Fig. 2-B.

The CMn-Fe nps magnetization, induced by an ap-

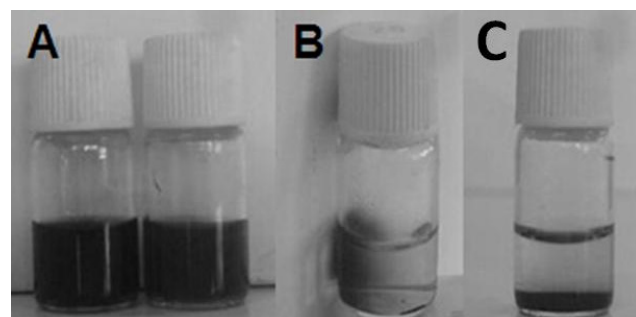


Fig. 1: Mn-Fe nps samples before (A) and after imposing an external magnetic field in the left (B) and under (C) of vial wall

plied magnetic field, increased with increasing applied field strength and reached a saturation magnetization value of 95 emu/g. The results were shown in Fig. 3.

### MRI Imaging

The MRI images (T2 imaging) of the mice before and 4 hours after injection of CMn-Fe nps were shown in Fig. 4. The liver and some other organs were accumulated the CMn-Fe nps particles and produced a negative contrast in images. The imaging from the extraction tissues showed that nanoparticles were existed in blood and liver at 10 minutes after injection. At 4 hours after injection, the nanoparticles were seen in liver, spleen and kidneys but washed from the blood.

Iron determination was performed in organs by tissue extraction. The results are presented in Fig. 5 as percent of iron (g) injected per gram of dry tissues. At

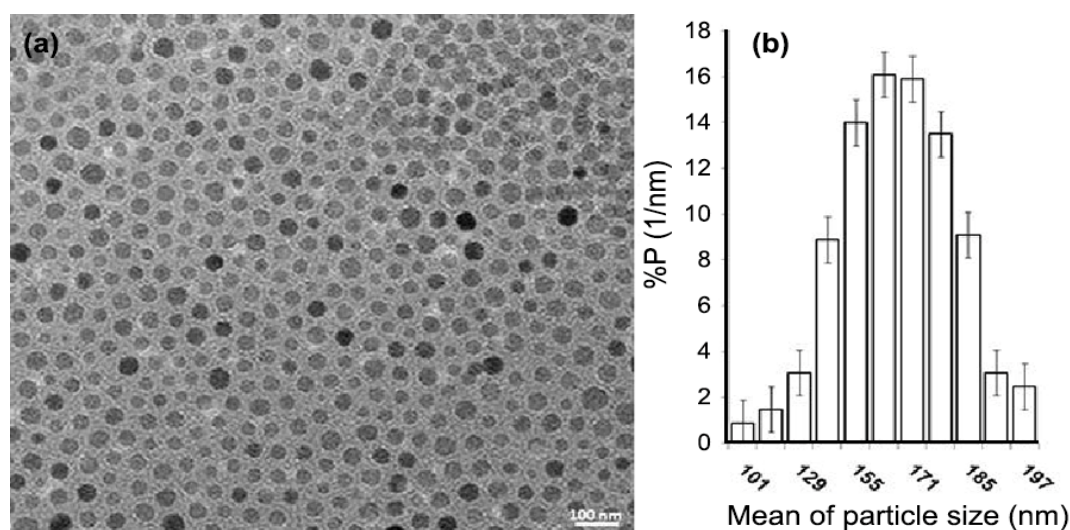


Fig. 2: TEM image shows the core size of Mn-Fe nps is  $54\pm 27$  nm (A). Mn-Fe nps hydrodynamic size distribution (mean  $149\pm 48$  nm) determined by dynamic light scattering technique (B)

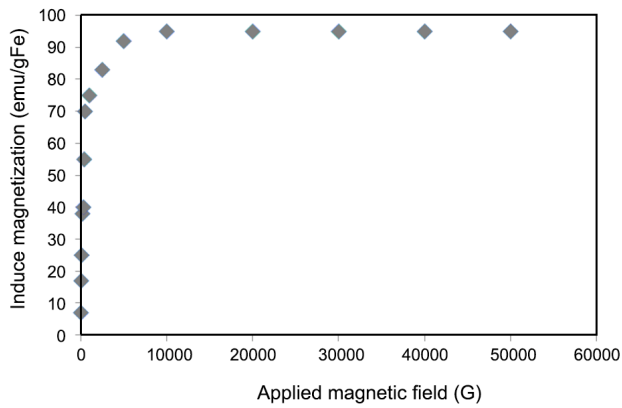


Fig. 3: CMn-Fe nps magnetization curve measured by SQUID exhibiting magnetic saturation

48 h after administration of the HMNs, the difference of iron concentration in organs and tumor was compared with and without external instant magnetic field. The results are shown in Fig. 5. The iron concentration in tumors was significantly increased (p-value < 0.05) by external magnetic field. While in other group, the higher concentration of iron was distributed in livers and spleens.

**Discussion**

In this work, CMn-Fe nps were synthesized, determined the physical characteristics and considered their biodistribution in some organs of normal mice such as liver, spleen, blood and kidneys with MRI imaging. The core size of CMn-Fe nps that measure by TEM was  $54 \pm 27$  nm and the hydrodynamic size was  $149 \pm 48$ , that determined by DLS technique. This size is appropriated for phagocyte by kupffer cells in liver. The nanoparticles with hydrodynamic radius larger than 80 nm are non-specifically taken up by kupffer cells in the healthy liver, allowing for hepatic imaging and diag-

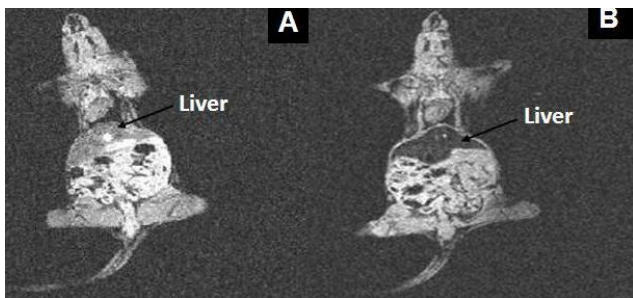


Fig. 4: The Comparison of mice liver before (A) and 4 hours after (B) CMn-Fe nps injection. The liver after absorption particles produced a negative contrast in MR images

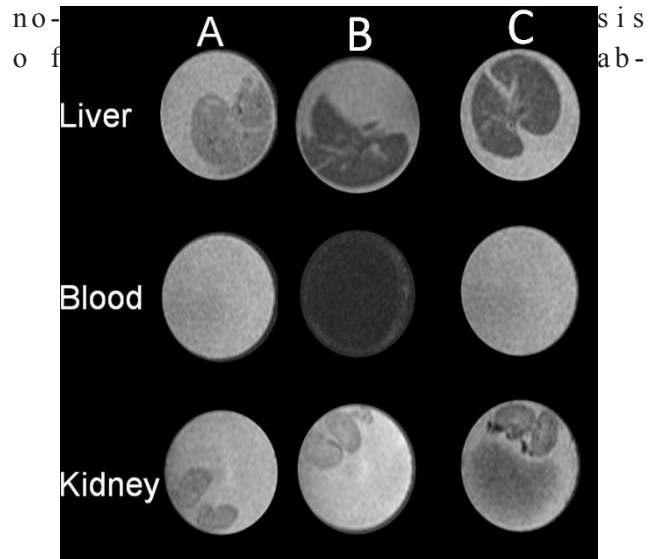


Fig. 5: The Comparison of mice liver, blood, kidneys and spleen before (A) 10 minutes (B) and 4 hours (C) after CMn-Fe nps injection

normality in liver, spleen and macrophage cell. The magnetization reached a saturation magnetization value of 95 emu/g. The MRI imaging results showed that the spleen and liver kupffer cells can absorb CMn-Fe nps very easily and produce a negative contrast in images. In 2013, Lopez and *et al.*, synthesized chitosan iron oxide nanoparticles in Microemulsion method. The core size of their magnetic nanoparticles was 50 nm with TEM images and the magnetization value was 49–53 emu/g (Lopez, *et al.*, 2013). In a study, the potential of chitosan coated ferrite nanoparticles were examined as an MRI contrast agent. The coating of chitosan was formed simultaneously with the synthesis of ferrite nanoparticles. A dynamic light-scattering spectrometer determined the average diameters of the coated nanoparticles at 67.0 nm. The animal experiment was performed in abdomen of a New Zealand rabbit with and without the injection of the aqueous solution of chitosan-coated nanoparticles by MR images. The ratio of the signal intensity showed the presence of the particles in the kupffer cell positions (Hong, *et al.*, 2010).

**CONCLUSIONS**

In this study, chitosan manganese-ferrite nanoparticles

were synthesized easily with good properties. The results showed that these nanoparticles can specially localize in the liver and spleen and produced a negative contrast in MRI images. Therefore we can conclude it is a good candidate for using as a contrast agent material in macrophage cells imaging with MRI.

## REFERENCES

- Banerjee, T.; Mitra, S.; Kumar Singh, A.; Kumar Sharma, R.; Maitra, A., (2002). Preparation, characterization and biodistribution of ultrafine chitosan nanoparticles, *Int. J. Pharm.* 243(1-2): 93-105.
- Dung, D.T.K.; Hai, T.H.; Phuc, L.H.; Long, B.D.; Vinh, L.K.; Truc, P.N., (2009). Preparation and characterization of magnetic nanoparticles with chitosan coating. *J. Phys.*, 187(1): 1-5.
- Gupta, A.K.; Gupta, M., (2005). Synthesis and surface engineering of iron oxide nanoparticles for biomedical applications, *Biomaterials*, 26(18): 3995-4021.
- Hong, S.; Chang, Y.; Rhee, I., (2010). Chitosan-coated ferrite (Fe<sub>3</sub>O<sub>4</sub>) nanoparticles as a T<sub>2</sub> contrast agent for magnetic resonance imaging. *J. Korean Phys. Soc.*, 56(3): 868-873.
- Hritcu, D.; Popa, M.I.; Popa, N.; Badescu, V.; Balan, V., (2009). Preparation and characterization of magnetic chitosan nanospheres. *Turk. J. Chem.*, 33: 785-796.
- Ito, A.; Shinkai, M.; Honda, H.; Kobayashi, T., (2005). Medical application of functionalized magnetic nanoparticles. *J. Biosci. Bioeng.*, 100(1): 1-11.
- Kueny-Stotz, M.; Garofalo, A.; Felder-Flesch, D., (2012). Manganese-Enhanced MRI Contrast Agents: From Small Chelates to Nanosized Hybrids. *Eur. J. Inorg. Chem.*, 2012(12): 1987-2005.
- Lopez, R.G.; Pineda, M.G.; Hurtado, G.; Diaz de Leon, R.; Fernandez, S.; Saade, H.; Bueno, D., (2013). Chitosan-Coated Magnetic Nanoparticles Prepared in One Step by Reverse Microemulsion Precipitation. *Int. J. Mol. Sci.*, 14(10): 19636-19650.
- Patil, R.M.; Shete, P.B.; Thorat, N.D.; Otari, S.V.; Barick, K.C.; Prasad, A.; Ningthoujam, R.S.; Tiwale, B.M.; Pawar, S.H., (2014). Superparamagnetic iron oxide/chitosan core/shells for hyperthermia application: Improved colloidal stability and biocompatibility. *J. Magn. Magn. Mater.*, 355: 22-30.
- Qu, J.; Liu, G.; Wang, Y.; Hong, R., (2010). Preparation of Fe<sub>3</sub>O<sub>4</sub>-chitosan nanoparticles used for hyperthermia. *Adv. Powder Technol.*, 21(4): 461-467.
- Rasaneh, S.; Dadras, M.R., (2014). Detection of Her2 levels in cancerous cells based on iron oxide nanoparticles. *Int. J. Bio-Inorg. Hybr. Nanomater.*, 3(3): 157-162.
- Rasaneh, S.; Rajabi, H.; Babaei, M.H.; Akhlaghpour, S., (2011). MRI contrast agent for molecular imaging of the HER2/neu receptor using targeted magnetic nanoparticles. *J. Nanopart. Res.*, 13(6): 2285-2293.
- Thorek, D.L.J.; Chen, A.K.; Czupryna, J.; Tsourkas, A., (2006). Superparamagnetic Iron Oxide Nanoparticle Probes for Molecular Imaging. *Ann. Biomed. Eng.*, 34(1): 23.
- Wang, J.J.; Zeng, Z.W.; Xiao, R.Z.; Xie, T.; Zhou, G.L.; Zhan, X.R., (2011). Recent advances of chitosan nanoparticles as drug carriers. *Int. J. Nanomedicine*, 6: 765-774.

## AUTHOR (S) BIOSKETCHES

**Samira Rasaneh**, Assistant Professor, Nuclear Sciences and Technology Research Institute, Tehran,  
*E-mail: srasaneh@aeoi.org.ir*

**Maryam Raheleh Dadras**, M.Sc., International Campus, Iran University of Medical Sciences, Tehran